

Provided for non-commercial research and education use.  
Not for reproduction, distribution or commercial use.



This article appeared in a journal published by Elsevier. The attached copy is furnished to the author for internal non-commercial research and education use, including for instruction at the authors institution and sharing with colleagues.

Other uses, including reproduction and distribution, or selling or licensing copies, or posting to personal, institutional or third party websites are prohibited.

In most cases authors are permitted to post their version of the article (e.g. in Word or Tex form) to their personal website or institutional repository. Authors requiring further information regarding Elsevier's archiving and manuscript policies are encouraged to visit:

<http://www.elsevier.com/copyright>



Contents lists available at SciVerse ScienceDirect

Journal of Membrane Science

journal homepage: [www.elsevier.com/locate/memsci](http://www.elsevier.com/locate/memsci)

## Solid state, dry zinc/MCM-41/air cell as relative humidity sensor

Hens Saputra<sup>a</sup>, Raihan Othman<sup>b,\*</sup>, A.G.E. Sutjipto<sup>b</sup>, R. Muhida<sup>b</sup>, M.H. Ani<sup>b</sup>

<sup>a</sup> Pusat Teknologi Industri Proses, Badan Pengkajian dan Penerapan Teknologi (BPPT), Jl. M.H. Thamrin No. 8, Jakarta 10340, Indonesia

<sup>b</sup> Faculty of Engineering, International Islamic University Malaysia, P.O. Box 10, 50728 Kuala Lumpur, Malaysia

### ARTICLE INFO

#### Article history:

Received 15 October 2011

Received in revised form

20 April 2012

Accepted 1 May 2012

Available online 11 May 2012

#### Keywords:

MCM-41 separator

Inorganic ion-exchange membrane

Zn/MCM-41/air cell

Solid state cell

Relative humidity sensor

### ABSTRACT

A zinc–air cell utilizing an inorganic MCM-41 membrane separator, in its dry form, reveals a unique behavior in response to relative humidity variation. The open circuit voltage (OCV) of the cell shows a linear dependence on relative humidity content. This is due to water adsorption–desorption characteristics of the mesoporous MCM-41 material. Comparison between relative humidity data obtained from commercial digital humidity sensor with data deduced from the OCV readings of Zn/MCM-41/air cell shows good sensitivity and high reliability.

© 2012 Elsevier B.V. All rights reserved.

### 1. Introduction

The MCM-41 material belongs to a group of mesoporous materials known as M41S. This class of materials is characterized by its hexagonally ordered, uniform nano-channels with large surface area [1–3]. The MCM-41 material has found vast applications particularly in membrane filtration technology [4–7]. Recently, we introduced MCM-41 as a new separator material for electrochemical cells and demonstrated its viability in a zinc–air cell [8]. Unlike the polymeric separator, the MCM-41 membrane separator assumes three roles simultaneously, namely (i) preventing electronic contact between anode and cathode, (ii) permitting ionic exchange between anolyte and catholyte through its nano-channels, and (iii) serving as an electrolyte reservoir matrix utilizing its hydrophilic, porous structure.

The MCM-41 surface structure is covered with silanol groups (Si-OH) formed during the synthesis of the material [9,10]. The hydrophilic characteristic of the material is attributed to the existence of these Si-OH groups. When applied as a membrane separator in the zinc–air cell, the MCM-41 materials high adsorption affinity towards water leads to a unique behavior of the cell. The open circuit potential value of the cell, in its dry form without the inclusion of electrolyte, is found to be responsive and distinctive to the humidity content and thus enables it to be utilized as a novel relative humidity sensor. The present work

reports the findings of this unique characteristic of Zn/MCM-41/air cell.

Humidity sensors are based on a wide range of transduction principles such as capacitive, resistive, hygrometric, gravimetric and optical ones [11,12]. Among these, the capacitive technique is the most common since it is relatively inexpensive and the transduction mechanism is very specific to humidity [11,12]. In principle, a hygroscopic polymer or a ceramic material placed in between two parallel plates of capacitor and as humidity varies the dielectric constant of the hygroscopic material changes as well. As a result the humidity-dependent capacitance becomes the quantifying parameter for humidity. The capacitive transducer, however, requires power to operate. The Zn/MCM-41/air electrochemical sensor of this work, on the other hand, generates voltage (e.m.f.) and its value becomes a measurable parameter for humidity.

### 2. Experimental

#### 2.1. Synthesis and characterization of MCM-41 material

The MCM-41 material was synthesized from a sol–gel route. The parent solution for synthesis consisted of the molar ratio formulation 1.0TEOS:0.05CTAB:0.5NaOH:100H<sub>2</sub>O. Tetraethylorthosilicate (TEOS) served as the silicon source while the cetyltrimethyl ammonium bromide (CTAB) cationic surfactant was the organic template. The preparation procedure was as follows. CTAB was dissolved in distilled water and sodium hydroxide (NaOH) under stirring at 200 rpm for 15 min at room temperature, and followed by addition

\* Corresponding author. Tel.: +60 3 61964561; fax: +60 3 61964853.

E-mail addresses: [raihan@iiu.edu.my](mailto:raihan@iiu.edu.my), [raihan\\_othman@yahoo.com](mailto:raihan_othman@yahoo.com) (R. Othman).

of TEOS. The stirring process was continued for another 30 min before finally obtaining the parent solution. A zinc substrate was then dipped into the parent solution and air dried. This procedure can be repeated to prepare an MCM-41 coating to the desired thickness. The surfactant was finally removed from the pores structure by leaching with ethanol.

The structural formation of MCM-41 onto zinc substrate was verified using X-ray diffraction (Cu K $\alpha$  radiation, a scan range of 2–80° 2 $\theta$  and scan speed of 2° min<sup>-1</sup>).

### 2.2. Fabrication of Zn/MCM-41/air cell

The cell comprised of zinc foil (99.9%, 250  $\mu$ m thick) which has been coated by MCM-41 membrane as the anode and a commercially available air cathode sheet. The air electrode consisted of laminated structures of fibrous carbon and sandwiched against a nickel mesh support. The air-side of the electrode is covered with a gas permeable, hydrophobic Teflon layer. Fig. 1 shows a schematic drawing of the Zn/MCM-41/air cell. The complete cell dimensions were 1 cm<sup>2</sup> area  $\times$  ca. 450  $\mu$ m thickness.

### 2.3. Fabrication of Zn/disordered silica/air cell

In order to substantiate the unique role of MCM-41 in producing Zn/air cell sensing characteristics, a disordered silica separator material was also utilized. Disordered silica was prepared using tetraethylorthosilicate (TEOS) as the source of silica, water and

ethanol (C<sub>2</sub>H<sub>5</sub>OH) as solvents and hydrochloric acid (HCl) as catalyst, with the molar ratio formulation 1:3:0.35:6 (TEOS:C<sub>2</sub>H<sub>5</sub>OH:HCl:H<sub>2</sub>O). The parent solution was stirred at 250 rpm for 1 h and heated to 50 °C, forming a semi-gel phase. The zinc electrode was then coated with the silica material by the dip coating procedure and fabricated into a Zn/air cell, as described earlier.

### 2.4. Monitoring cell OCV as a function of relative humidity

Fig. 2 illustrates the experimental setup to measure the OCV of Zn/MCM-41/air cell under different humidity contents. Varying humidity content was achieved by controlling the gas flow rate ratio between the wet inlet gas and the dry inlet gas, i.e. P/P<sup>0</sup>. The dry inlet gas was obtained by pumping the ambient air through two stages silica water trap while the wet inlet gas was obtained by pumping the ambient air through a two stages humidifier or water bath. P/P<sup>0</sup> values were varied from 0 (i.e. when the wet gas inlet Q<sub>1</sub> was closed) until 1 (i.e. when the dry gas inlet Q<sub>0</sub> was closed). P/P<sup>0</sup> values were then calibrated against relative humidity readings from a digital humidity sensor (Lascar Humidity EL-USB-2). The OCV of the cell was monitored online using an Eco Chemie (The Netherlands) Autolab Galvanostat/Potentiostat. P/P<sup>0</sup> value was changed only after stabilization in the OCV, which was observed for at least an hour. OCV readings of the Zn/MCM-41/air cell were recorded during both humidification and dehumidification profiles.

## 3. Results and discussion

The structural formation of MCM-41 membrane onto zinc substrate was confirmed by the XRD pattern as shown in Fig. 3. MCM-41 material large *d*-spacing is characterized by low angle diffractions, i.e. high intensity (100) peak at 2 $\theta$ ~2° and followed by three small peaks of (110), (200) and (210) which are normally suppressed [13]. The rest of the peaks are attributed to the zinc element. The MCM-41 material consists of one dimensional, hexagonally-ordered pore structure with a narrow pore size distribution which centered around 2 nm [1–3]. Its nanoporous

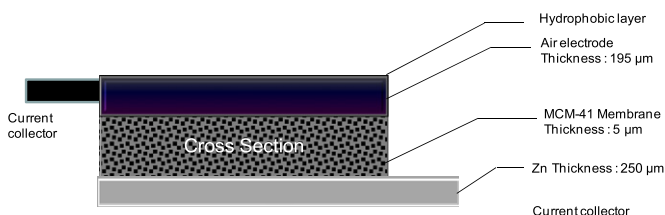


Fig. 1. Schematic illustration of Zn/MCM-41/air cell design.

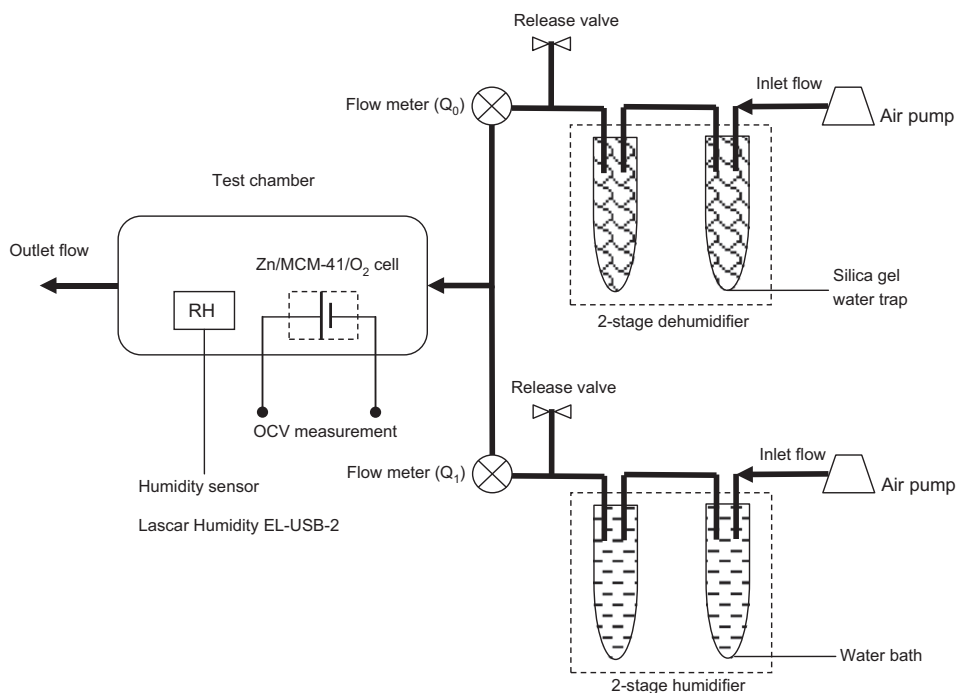


Fig. 2. Experimental setup for OCV measurement of Zn/MCM-41/air cell with varying relative humidity content.

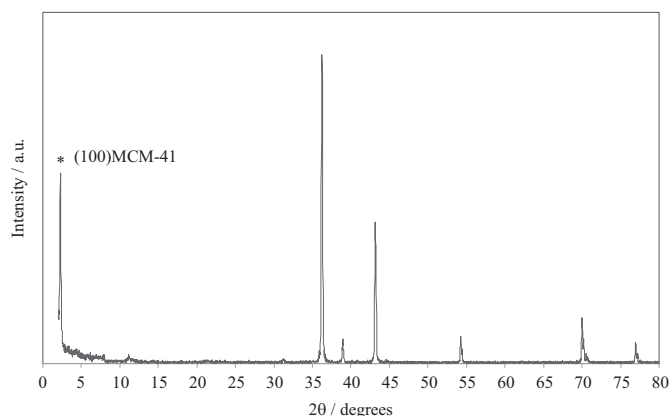


Fig. 3. X-ray diffractions confirming the formation of MCM-41 membrane onto zinc anode.

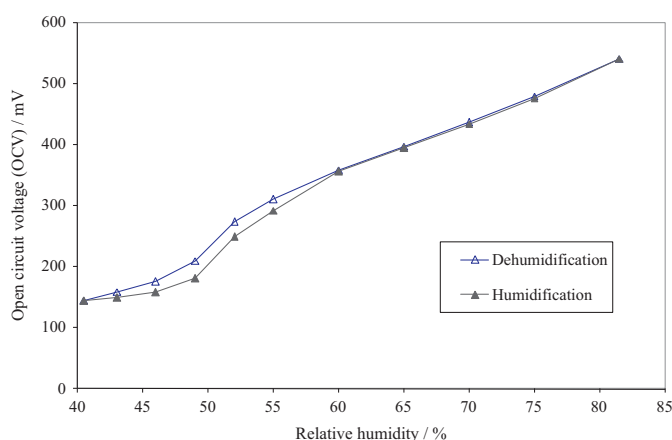


Fig. 4. OCV response of Zn/MCM-41/air cell as a function of relative humidity.

matrix contributes towards the high surface area and high pore volume characteristics. Repeated measurements from earlier work have ascertained that the BET surface area and pore volume density of as-synthesized MCM-41 were  $1200 \text{ m}^2\text{g}^{-1}$  and  $1.08 \text{ cm}^3\text{g}^{-1}$ , respectively [4,5].

Fig. 4 illustrates the OCV response of Zn/MCM-41/air cell to relative humidity. The experimental setup managed to simulate relative humidity content between 40 and 80% which sufficed to characterize local weather conditions. Simulation to lower or higher humidity contents could be achieved simply by adding more humidity trap or humidifier bath, respectively. The cell OCV values were found responsive to humidity content during both humidification and dehumidification profiles. A linear correlation was observed for humidity content in the range 60–80%. In fact the regression factor  $R^2$  value was 0.99 for this region, indicating a very good linear correlation. Thus if the cell OCV ( $V_{oc}$ ) registered value is equal to or greater than 350 mV, the relative humidity value (H) can be deduced from the linear relation

$$V_{oc} = mH(\%) + V_{int}; \quad V_{oc} \geq 350 \text{ mV} \quad (1)$$

or

$$H(\%) = \frac{V_{oc} - V_{int}}{m}; \quad V_{oc} \geq 350 \text{ mV} \quad (2)$$

where  $m$  and  $V_{int}$  are the regression constants.

Hysteresis occurs for humidity content less than 60% and the OCV variation between humidification and dehumidification profiles was the largest at around 50% humidity content. The phenomena can be

explained from the water adsorption–desorption characteristics of MCM-41 material as shown in Fig. 5 [14]. The hysteresis pattern and steep increase at relative vapor pressure between 0.5 and 0.6 are the characteristics of mesoporous materials [3,15,16]. The hysteresis occurred due to inner pores having larger diameter than the middle pores (i.e. slit structure), causing slower desorption process. This characteristic explains the hysteresis in the OCV response, i.e. slower water desorption contributes to higher OCV values during the dehumidification process.

In order to substantiate the findings, the relative humidity of our laboratory was monitored continuously for 48 h utilizing a digital humidity sensor (Lascar Humidity EL-USB-2) and also the Zn/MCM-41/air cell by measuring its OCV. The OCV readings were then converted into relative humidity values using Eq. (2). Fig. 6 illustrates the comparison between the two sets of data obtained, showing a significant correlation. Take note that the humidity variation for the duration of test was between 65% and 80% which lies in the linear region of the OCV calibration plot of Fig. 4. We also anticipate a linear dependence of OCV values on humidity content for humidity less than 45%. This is supported by the converging trend of humidification and dehumidification profiles of OCV calibration plot and also the water adsorption–desorption characteristics of MCM-41 material. As for the humidity content between 45% and 60%, though a linear dependence was not observed, the system could be calibrated with known humidity content.

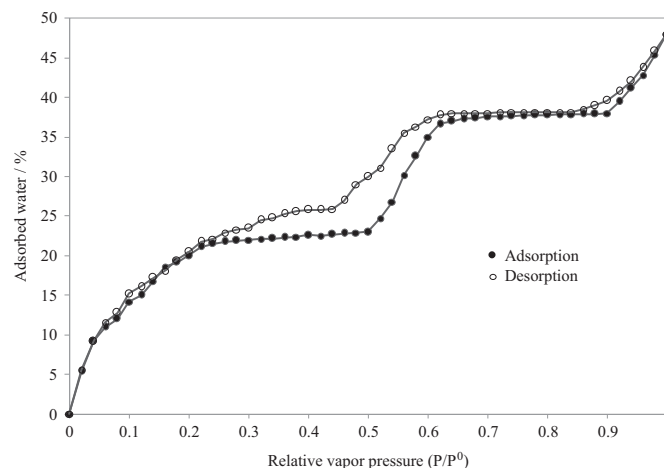


Fig. 5. Water adsorption–desorption characteristics of MCM-41 material, after [12].

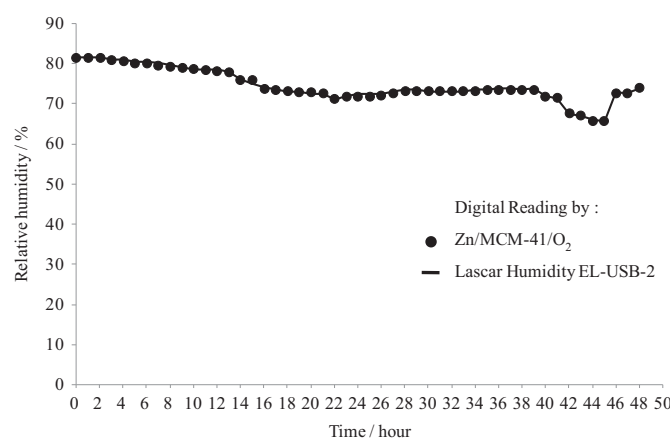
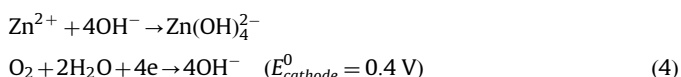
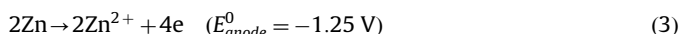


Fig. 6. Relative humidity measurement utilizing a digital humidity sensor and OCV readings from the Zn/MCM-41/air cell.

A Zn/air cell was also fabricated using disordered silica (DS) as the membrane separator material and its OCV measured against relative humidity of the ambient surrounding. Fig. 7 depicts the OCV readings of Zn/MCM-41/air cell and Zn/DS/air cell, as compared to relative humidity variation (% RH). It clearly supports the unique role contributed by MCM-41 material which resulted in humidity sensing behavior of Zn/MCM-41/air cell. Initially the OCV value of Zn/DS/air cell increased with increasing humidity but later remained constant with changing humidity.

MCM-41 high adsorption affinity towards water is attributed to the existence of silanol group (Si-OH) covering the surface structure of the material. There are in fact different kinds of silanol groups in MCM-41, denoted by  $Q^{4-n}$ , where  $n$  refers to the number of hydroxyl groups attached to a silicon atom [17]. Mainly there are three distinct silanol groups, namely,  $Q^2$   $[(SiO)_2(Si-OH)_2]$ ,  $Q^3$   $[(SiO)_3Si-OH]$  and  $Q^4$   $[(SiO)_4]$ . In all these groups, silicon has a tetrahedral arrangement bonding with four atoms. The  $Q^4$  group is mainly located within the pore wall of MCM-41. The  $Q^2$  group contributes only around 3–5% of the total number of Q groups in MCM-41. The most dominant is  $Q^3$  which is responsible for the water absorption property and serves as the hydration site. This group forms 40–60% of the silanol group [10,18]. The hydrophilic characteristic of MCM-41 material is attributed to this type of silanol group. When water molecules are introduced to the surface of MCM-41, they will initially attach to the Si-OH hydration sites through hydrogen bonds. Later, hydrogen bonded clusters of water molecule may begin to form as water molecules bond to the previously adsorbed water [19], as illustrated in Fig. 8. It is suggested that the hydroxyl groups are pointing towards the center of MCM-41 pore channels [6]. As a result, during drying most water molecules left the pores but prior to reaching the final drying stage, the water molecules re-distributed into a monolayer covering the wall of the pores, maintaining a low hydration level in the MCM-41 material [20].

An alkaline zinc–air cell is characterized by the following redox couple [21]:



Thus, the open circuit potential ( $V_{oc}$ ) of the cell is related to the activities of the reacting species ( $a_i$ ) by the Nernst relationship [22,23]

$$V_{oc} = (E_{cathode}^0 - E_{anode}^0) - \frac{RT}{zF} \ln \left( \frac{a_{Zn}^2 a_{OH^-}^4}{a_{Zn^{2+}} a_{H_2O}^2 p_{O_2}} \right) \quad (5)$$

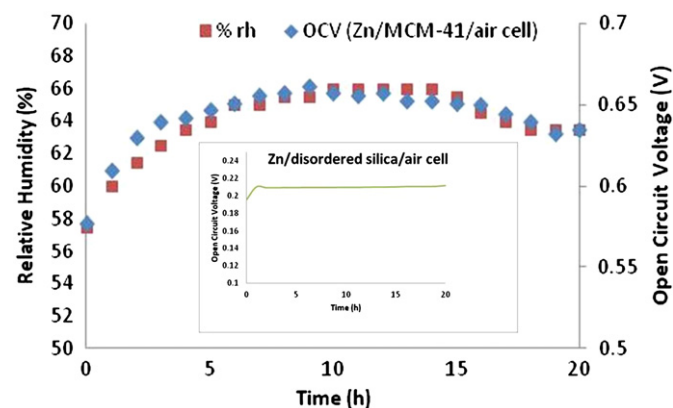


Fig. 7. OCV readings of Zn/MCM-41/air cell against relative humidity content as compared to the OCV variation of Zn/disordered silica/air cell (inset).

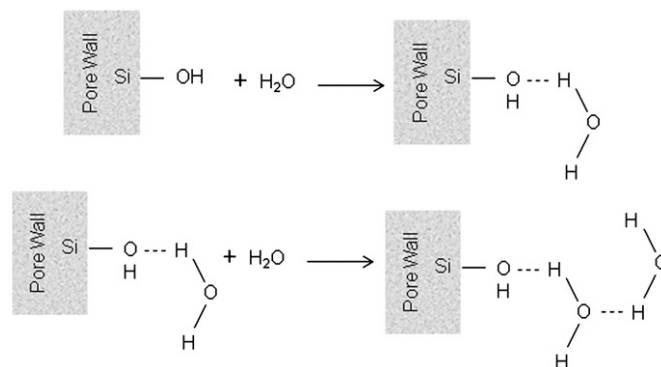


Fig. 8. Water molecules adsorption mechanisms in MCM-41 pore wall surrounding.

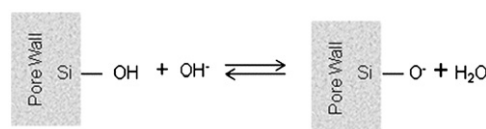


Fig. 9. Schematic illustration of interaction of water molecule and the pore wall.

$$V_{oc} = 1.65 - \frac{RT}{4F} \ln \left( \frac{a_{Zn^{2+}}^2 a_{OH^-}^4}{a_{H_2O}^2 p_{O_2}} \right) \quad (6)$$

where  $R$ ,  $T$ ,  $F$  and  $z$  are the gas constant, absolute temperature, Faraday constant and number of electrons exchanged, respectively. In the above formula, the activity of Zn ( $a_{Zn}$ ) is taken as unity since it is a pure substance and the activity of  $O_2$  is taken as its partial pressure ( $p_{O_2}$ ). However, in the present case of ‘dry’ Zn/MCM-41/air cell, the activity of water solvent  $a_{H_2O}$  cannot be taken as unity as the presence of water solvent is merely in the form of adsorbed moisture from the ambient air. Consequently, the activities of zinc and hydroxyl ions ( $a_{Zn^{2+}}$ ,  $a_{OH^-}$ ) also depend on the water activity. It is believed that moisture absorbed from the ambient air activates hydroxyl ( $OH^-$ ) ions from the pore wall and along with the  $OH^-$  ions is entrapped within the pore channels [24,25]. Fig. 9 gives a schematic illustration of the activation of  $OH^-$  ions from the pore wall. Thus water adsorption–desorption characteristics of MCM-41 material induces the variation in the OCV of Zn/MCM-41/air cell. This is further supported by the fact that oxygen reduction activity can be observed even in quasi-neutral electrolytes [26–28]. The more the moisture content absorbed, the higher the cell OCV due to the increase in water activity. As a result the variation in Zn/MCM-41/air cell’s OCV could then be used as a measure of relative humidity content.

#### 4. Conclusion

Zn/MCM-41/air cell in its dry form generates OCV once exposed to ambient air moisture and the value is found to be responsive and distinctive to relative humidity content. It is believed that the moisture, absorbed from the ambient air due to MCM-41 material’s high adsorption affinity towards water, activates hydroxyl ions from the pore wall and within the pore channels of the structure. The unique water adsorption–desorption characteristics of MCM-41 material influences the adsorbed water activity which in turn induces the variation in the cell’s OCV. Consequently the Zn/MCM-41/air system can be effectively utilized as a novel relative humidity sensor.

## Acknowledgment

The International Islamic University Malaysia funded this project through the Research Matching Grant Scheme (RMGS 09–09). The authors gratefully acknowledge the financial support.

## References

- [1] C.T. Kresge, M.E. Leonowicz, W.J. Roth, J.C. Vartuli, J.S. Beck, Ordered mesoporous molecular sieves synthesized by a liquid-crystal template mechanism, *Nature* 359 (1992) 710–712.
- [2] J.S. Beck, J.C. Vartuli, W.J. Roth, M.E. Leonowicz, C.T. Kresge, K.D. Schmitt, C.T.W. Chu, D.H. Olson, E.W. Sheppard, A new family of mesoporous molecular sieves prepared with liquid crystal templates, *J. Am. Chem. Soc.* 114 (1992) 10834–10843.
- [3] A.J. Burggraaf, L. Cot, *Fundamentals of Inorganic Membrane Science and Technology*, Elsevier, Amsterdam, 1996.
- [4] N. Nishiyama, H. Saputra, D.H. Park, Y. Egashira, K. Ueyama, Zirconium-containing mesoporous silica Zr–MCM-48 for alkali resistant filtration membranes, *J. Membr. Sci.* 218 (2003) 165–171.
- [5] D.H. Park, H. Saputra, N. Nishiyama, Y. Egashira, K. Ueyama, Synthesis of zirconium-containing mesoporous silica Zr–MCM-48 membranes with high alkaline resistance for nanofiltration, *Stud. Surf. Sci. Catal.* 146 (2003) 327–330.
- [6] Z. Tang, P. Sheng, *Nanoscience and Technology: Novel Structure and Phenomena*, Taylor & Francis Inc., London, 2003.
- [7] S.A. Bagshaw, F. Testa, Wairakei geothermal silica, a low cost reagent for the synthesis of mesostructured M41S alumino-silicate molecular sieves, *Microporous Mesoporous Mater.* 39 (2000) 67–75.
- [8] H. Saputra, R. Othman, A.G.E. Sutjipto, R. Muhida, MCM-41 as a new separator material for electrochemical cell: application in zinc–air system, *J. Membr. Sci.* 367 (2011) 152–157.
- [9] X.S. Zhao, G.Q. Lu, Modification of MCM-41 by surface silylation with trimethylchlorosilane and adsorption study, *J. Phys. Chem. B* 102 (1998) 1556–1561.
- [10] X.S. Zhao, G.Q. Lu, A.K. Whittaker, G.J. Millar, H.Y. Zhu, Comprehensive study of surface chemistry of MCM-41 using  $^{29}\text{Si}$  CP/MAS NMR, FTIR, Pyridine-TPD, and TGA, *J. Phys. Chem. B* 101 (1997) 6525–6531.
- [11] Z.M. Rittersma, Recent achievements in miniaturised humidity sensors—A review of transduction techniques, *Sens. Actuators A* 96 (2002) 196–210.
- [12] Z. Chen, C. Lu, Humidity sensors: a review of materials and mechanisms, *Sens. Lett.* 3 (2005) 274–295.
- [13] L. Jia, A. Katiyara, N.G. Pintoa, M. Jaroniec, P.G. Smirniotis, Microporous Mesoporous Mater 75 (2004) 221–229.
- [14] H. Saputra, *Synthesis and Characterization of Zirconium-containing Nanoporous Silica Membranes*, M.Sc. Thesis, Osaka University, Japan, 2003.
- [15] P.J. Branton, P.G. Hall, K.S.W. Sing, Physisorption of alcohols and water vapour by MCM-41, a model mesoporous adsorbent, *Adsorption* 1 (1995) 77–82.
- [16] H.G. Karge, J. Weitkamp, *Molecular Sieves 1*, Springer, Netherlands, 1998.
- [17] D. Baute, V. Frydman, H. Zimmermann, Sh. Kababya, D. Goldfarb, Properties of the silica layer during the formation of MCM-41 studied by EPR of a silica-bound spin probe, *J. Phys. Chem. B* 109 (2005) 7807–7816.
- [18] J. Rathousky, M. Zukalova, A. Zukal, J. Had, Homogeneous precipitation of siliceous MCM-41 and bimodal silica, *Collect. Czech. Chem. Commun.* 63 (1998) 1893–1906.
- [19] Y. Long, T. Xu, Y. Sun, W. Dong, Adsorption behavior on defect structure of mesoporous molecular sieve MCM-41, *Langmuir* 14 (1998) 6173–6178.
- [20] Z. Tun, P.C. Mason, Observation of adsorption of water in MCM-41 with neutron diffraction, *Langmuir* 18 (2002) 975–977.
- [21] C. Chakkaravarthy, A.K. Abdul Waheed, H.V.K. Udupa, Zinc–air alkaline batteries—a review, *J. Power Sources* 6 (1986) 203–228.
- [22] J.P. Hoare, *The Electrochemistry of Oxygen*, John Wiley and Sons, Inc., 1968.
- [23] P.R. Roberge, *Handbook of Corrosion Engineering*, The McGraw-Hill Companies, 2000.
- [24] M. Hosokawa, K. Nogi, M. Naito, T. Yokoyama, *Nanoparticle Technology Handbook*, Elsevier, Netherland, 2007.
- [25] M. Nogami, R. Nagao, C. Wong, Proton conduction in porous silica glasses with high water content, *J. Phys. Chem. B* 102 (1998) 5772–5775.
- [26] J. Jindra, J. Mrha, M. Musilová, Zinc–air cell with neutral electrolyte, *J. Appl. Electrochem.* 3 (1973) 297–301.
- [27] A. Kozawa, V.E. Zilionis, R.J. Brodd, Oxygen and hydrogen peroxide reduction at a ferric phthalocyanine-catalyzed graphite electrode, *J. Electrochem. Soc.* 117 (1970) 1470–1474.
- [28] A. Kozawa, V.E. Zilionis, R.J. Brodd, Electrode materials and catalysts for oxygen reduction in isotonic saline reduction, *J. Electrochem. Soc.* 117 (1970) 1470–1474.